## DNA-tension dependence of restriction enzyme activity reveals mechanochemical properties of the reaction pathway

van den Broek, B.; Noom, M.C.; Wuite, G.J.L.

***published in***
Nucleic Acids Research
2005

***DOI (link to publisher)***
10.1093/nar/gki565

***document version***
Publisher's PDF, also known as Version of record

*2676–2684* *Nucleic Acids Research, 2005, Vol. 33, No. 8*
*doi:10.1093/nar/gki565*

# DNA-tension dependence of restriction enzyme activity reveals mechanochemical properties of the reaction pathway

**Bram van den Broek, Maarten C. Noom and Gijs J. L. Wuite***

Laser Centre and Department of Physics and Astronomy, Vrije Universiteit, Amsterdam, 1081 HV, The Netherlands

Received February 8, 2005; Revised April 8, 2005; Accepted April 21, 2005

## ABSTRACT

**Type II restriction endonucleases protect bacteria against phage infections by cleaving recognition sites on foreign double-stranded DNA (dsDNA) with extraordinary specificity. This capability arises primarily from large conformational changes in enzyme and/or DNA upon target sequence recognition. In order to elucidate the connection between the mechanics and the chemistry of DNA recognition and cleavage, we used a single-molecule approach to measure rate changes in the reaction pathway of EcoRV and BamHI as a function of DNA tension. We show that the induced-fit rate of EcoRV is strongly reduced by such tension. In contrast, BamHI is found to be insensitive, providing evidence that both substrate binding and hydrolysis are not influenced by this force. Based on these results, we propose a mechanochemical model of induced-fit reactions on DNA, allowing determination of induced-fit rates and DNA bend angles. Finally, for both enzymes a strongly decreased association rate is obtained on stretched DNA, presumably due to the absence of intradomain dissociation/re-association between non-specific sites (jumping). The obtained results should apply to many other DNA-associated proteins.**

## INTRODUCTION

Type II restriction endonucleases constitute an important defense mechanism of bacteria against viral attacks. Their function is to destroy invading foreign DNA molecules by catalyzing double-stranded DNA (dsDNA) breakage at certain recognition sequences. Discrimination between foreign and own DNA is established by an extreme selectivity in cleavage location (1–4). Such recognition sequences in the bacterial DNA are protected from cleavage by methylation of the site (5–7). Besides their indispensable usefulness as DNA scissors in molecular biology, the high specificity makes restriction enzymes important systems for studying specific protein–DNA interactions.

Restriction enzymes need to find their DNA target sequence as quickly as possible. Although driven by diffusion, this process can be faster than the 3D diffusion limit ($\sim 10^8$ $M^{-1}$ $s^{-1}$), suggesting that 1D diffusion along the DNA plays a role in target finding (8). Like many DNA-associated proteins, restriction enzymes can bind DNA non-specifically. This enables enzymes to 'scan' parts of the DNA during a random walk along its contour (9–13), thereby enhancing the search process. When a restriction enzyme recognizes a target sequence, it undergoes a large conformational change, sometimes inducing significant changes in the DNA structure as well. This induced-fit mechanism ensures the high sequence specificity of the enzymes (5,14–16). The rate of this process has not been measured but is estimated to be fast (17). Crystal structures of EcoRV bound to cognate DNA have, however, provided 'snapshots' of the induced-fit mechanism (2,18). In these studies, it has been shown that during the formation of a specific EcoRV–DNA complex divalent cations are trapped. At the same time, the active site residues are positioned in close proximity to the scissile phosphodiesters, preparing the enzyme for hydrolysis of the DNA backbone (Figure 1).

Type II restriction enzymes are often considered model systems for the mechanism proteins use to search specific DNA sites (12,13,19,20). At the same time, the sequence recognition by these enzymes is a typical example of an induced-fit mechanism. Numerous biochemical and structural studies have revealed a wealth of information about type II restriction enzymes (2–8,14–18,21–27). However, these studies have neither addressed the mechanochemistry in the reaction pathway, nor do they allow for the direct observation of the different reaction states. To clarify these aspects, we performed single-molecule experiments with EcoRV and BamHI, both recognizing a palindromic sequence 6 bp in length. These enzymes were chosen because of profound differences in DNA

*To whom correspondence should be addressed. Tel: +31205987987; Fax: +31205987991; Email: gwuite@nat.vu.nl

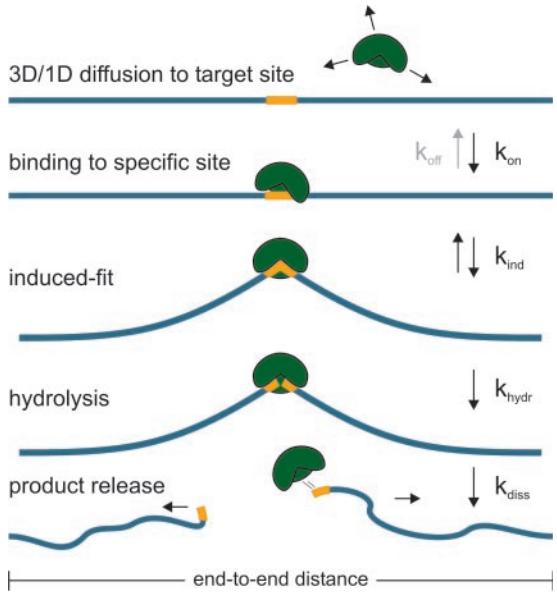


**Figure 1.** The reaction pathway for orthodox type IIP restriction endonucleases. The association rate $k_{on}$ is the only rate that depends on enzyme concentration. Under normal conditions, the induced-fit rate ($k_{ind}$) is much faster than hydrolysis ($k_{hydr}$) and product dissociation ($k_{diss}$). The applied tension $F$ opposes DNA bending by the enzyme in the induced-fit process.

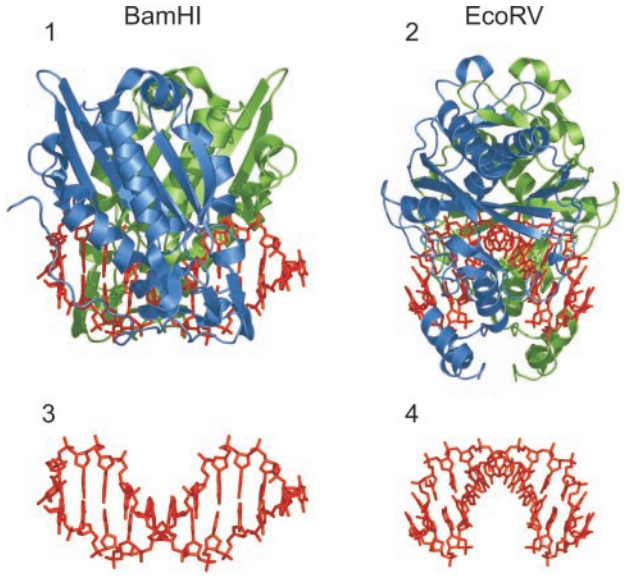


**Figure 2.** Crystal structures of specific enzyme–DNA complexes of BamHI (1) (23) and EcoRV (2) (2,18). The DNA configuration within both complexes is shown separately, (3) and (4), respectively. While BamHI does not distort its recognition site, EcoRV induces a 50° kink located at the center base pair step.

conformation in the specific complex; upon binding, EcoRV strongly deforms its target DNA, inducing a sharp kink of ~50° (2,18), whereas BamHI leaves the DNA practically in straight B-form (Figure 2) (3,22,23). Observation of restriction enzymes reacting with single DNA molecules allows for direct measurements of the searching and hydrolysis times. Moreover, the force dependence of these rates provides insight in the corresponding mechanochemistry (28–32) and permits determination of bend angles and induced-fit rates.

## MATERIALS AND METHODS

### Proteins and DNA

EcoRV endonuclease (gift from J. J. Perona) was purified and tested as described previously (17,33). A high concentration batch of BamHI purified by New England Biolabs was used. Plasmid *pCco5* DNA (6538 bp; gift from W. Reijnders, Vrije Universiteit, Amsterdam) was utilized for the single cleavage site experiments on EcoRV and BamHI, whereas for the multiple site experiments Lambda phage DNA (48 502 bp; Roche GmbH, Germany) was used. The *pCco5* plasmid was linearized by SpeI digestion (New England Biolabs) and extracted from 0.7% agarose gel using a QIAEX II kit (Qiagen). The linearized molecule contained one EcoRV site (GATATC), located in the middle. To create a construct with one BamHI site (GGATCC), the *pCco5* plasmid was digested by SpeI and NcoI, leaving a 4450 bp molecule with the BamHI site located at 1104 bp. The DNA fragments were incubated for 30 min at 37°C with 80 mM biotin-14-dATP and biotin-14-dCTP (Invitrogen), 100 mM dGTP and TTP (Sigma-Aldrich) and Klenow DNA Polymerase exo-minus (Fermentas) to label the 5′-overhangs. Excess nucleotides were removed with Microcon YM-10 filters (Millipore) in 10 mM Tris–HCl (pH 7.7). For the optical tweezers experiments, the biotin-labeled DNA was diluted to a concentration of ~1 pM in a 10 mM Tris–HCl (pH 7.7) buffer with 250 mM NaCl. The restriction enzyme buffer for both EcoRV and BamHI contains 100 mM NaCl, 1 mM 2-mercaptoethanol, 5 mM $MgCl_2$ and 10 mM Tris–HCl (pH 8.0).

### Experimental setup

A Nd:$YVO_4$ 1046 nm cw infrared laser (Millennia IR, Spectra Physics) was used to create two optical traps. The beam was expanded and split into two beams by a polarizing beam splitter. A telescope system was placed in one of the beam paths. The first of these two lenses was moveable by motorized micrometers (OMDC-2BJ, OptoSigma) in the plane perpendicular to the beam, allowing for accurate steering of the trap. The two beams slightly overfilled the back aperture of a high NA, water immersion objective (Plan Apo 60x/1.20 WI/DIC H, Nikon). Position and motion of the bead in the fixed trap was detected via back focal plane interferometry using a quadrant photodiode (34). Typical trap stiffness values achieved with a few hundred mW per trap are 100–200 pN/μm.

### Flow chamber

A custom-made flow system was used to flow in the solutions. Selection valves (Upchurch Scientific) were used to select the desired solution. Flow was generated by a high precision motorized syringe pump (Harvard Instruments). The flow chamber itself consisted of two parallel channels, where flow could be induced independently. The channels were connected to each other by a thin perpendicularly placed channel. In one channel, 2.17 or 1.87 μm streptavidin-coated beads (Spherotech) were stored, while the actual experiment took place in the other channel. When a DNA molecule was cut, new beads could be caught swiftly by directing flow from the bead channel via the connecting channel into the experiment channel.

When exchanging buffers, some mixing occurs at the interface between solutions. At the locus of the optical traps, it takes

several seconds before the solutions are fully exchanged. This was tested by flowing in dye while monitoring the change in illumination light transmission. The error of measuring the arrival time of a new solution was thus determined to be ~5 s. For experiments with high EcoRV and BamHI concentrations, a third flow channel containing these enzymes was added to improve the time resolution by a factor of 10. All experiments were conducted at room temperature (21°C).

## RESULTS

### Single-molecule experiments

The force dependence of the cleavage reaction of BamHI and EcoRV was determined as follows: dsDNA molecules with one or multiple recognition sequences were captured between two beads held by two optical traps, as described by Wuite *et al.* (35) (Figure 3). The DNA was put under tension by moving the position of one of the traps, while monitoring the force on the DNA. Enzymes were flowed in, preceded by buffer solution to remove excess DNA. Upon DNA cleavage, both beads recoiled back to the center of the traps, providing a clear signal for cleavage by an individual enzyme (Figure 4). The duration of a cleavage reaction is defined by the time elapsed between the arrival of the enzyme solution at the stretched DNA and DNA cleavage. Within this time span, an individual enzyme locates and binds the recognition site on the DNA, undergoes conformational changes to form the specific complex (the induced-fit mechanism), hydrolyses both DNA strands and eventually releases the product (Figure 1). By repeating this procedure at various forces, the average cleavage times as a function of DNA tension were obtained. Cleavage rates, $k_c$, were determined by taking the inverse of the average cutting times.

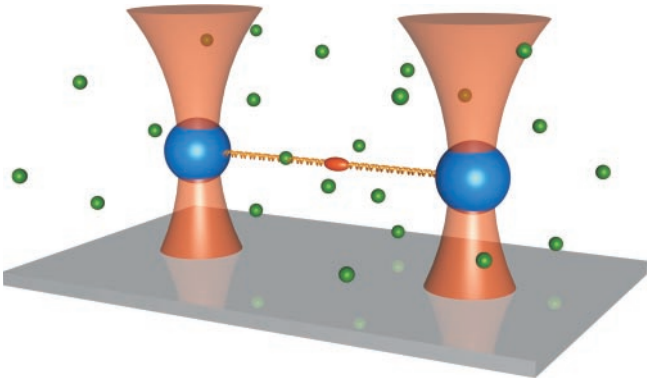

**Figure 3.** Schematic representation of the experimental approach. DNA (orange) is stretched between two beads (blue) trapped in optical tweezers. Enzymes (green spheres) in the solution diffuse in search of the recognition sequence (red).

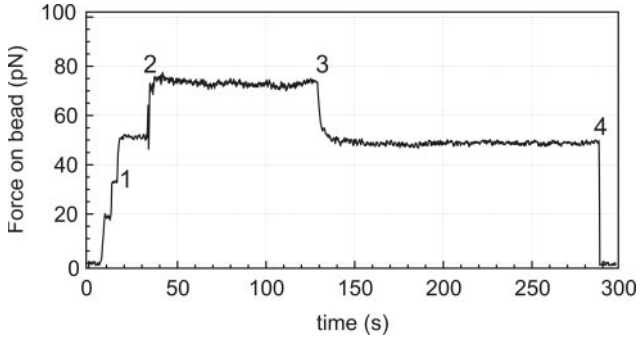


**Figure 4.** Typical data trace of a cleavage event. 1: Tension is being applied (in this case ~50 pN) and measured by the displacement of one of the trapped beads. 2: Start of enzyme flow. The drag force displaces the bead further from the center of the trap. The tension on the DNA molecule does not change, since both beads are influenced in the same way by the flow. 3: The flow is turned off. 4: The DNA is cleaved. Both beads recoil to the centers of the optical traps, instantly reducing the measured force to zero.

The results of these experiments with BamHI and EcoRV are shown in Figure 5. The data show that the observed EcoRV cleavage rate on linearized *pCco5* plasmid (number of recognition sites $n = 1$) decreases rapidly above of ~30 pN DNA tension (enzyme concentration 25 nM in terms of dimers) (Figure 5a). This decrease indicates that the tension induces another process in the cleavage reaction to become rate-limiting. Cleavage by 2.5 nM EcoRV of Lambda phage DNA ($n = 21$) also slows with tension, but the effect is much less prominent (Figure 5b). For BamHI, no such decrease is detected on either a *pCco5* derivative ($n = 1$) using an enzyme concentration of 300 nM or on Lambda phage DNA ($n = 5$) with 2.5 nM BamHI (Figure 5c). In contrast to other DNA enzymes (28,29), these restriction enzymes continue to function on DNA kept at high tensions. Even extending the DNA to halfway the overstretching plateau (~67 pN) (36) does not inhibit cleavage, presumably because part of the DNA molecule is still in dsDNA configuration. However, when DNA is fully overstretched to S-form (tension >70 pN), cleavage is completely blocked (measured with 500 nM EcoRV on Lambda phage DNA) (data not shown).

### Mechanochemistry of the reaction pathway

To explain why EcoRV and BamHI react differently to tension on the DNA, we assume that this tension primarily affects the induced-fit mechanism, because only during this process large conformational changes take place. A similar DNA tension dependence was also found for DNA polymerase (29).

Three independent energetic contributions can be identified in which DNA tension alters the free energy change in the induced-fit mechanism. These terms are pictured schematically in Figure 6a. First, tension on the DNA increases the average base pair spacing (enthalpic stretching) (37). Both EcoRV and BamHI tightly embrace the 6 bp compromising the recognition sequence. Furthermore, all amino acid–base contacts with the DNA are within this site and the base pair spacing is approximately the same as that of relaxed DNA (2,3,23). Therefore, the enthalpic stretching of these 6 bp needs to be suppressed by the enzyme. Second, an enzyme-induced kink directly shortens the DNA in the binding pocket against the applied force. The associated work has to be carried out by the enzyme. Third, the DNA protruding under an angle from the protein–DNA complex is bent in the direction of the force, which requires bending energy. Furthermore, it leads to an additional shortening of the end-to-end distance against the applied force. Both bending and shortening energies are paid by the enzyme during the induced-fit process. The actual amount of bending and shortening is a function of tension and can be calculated using the worm-like chain model for

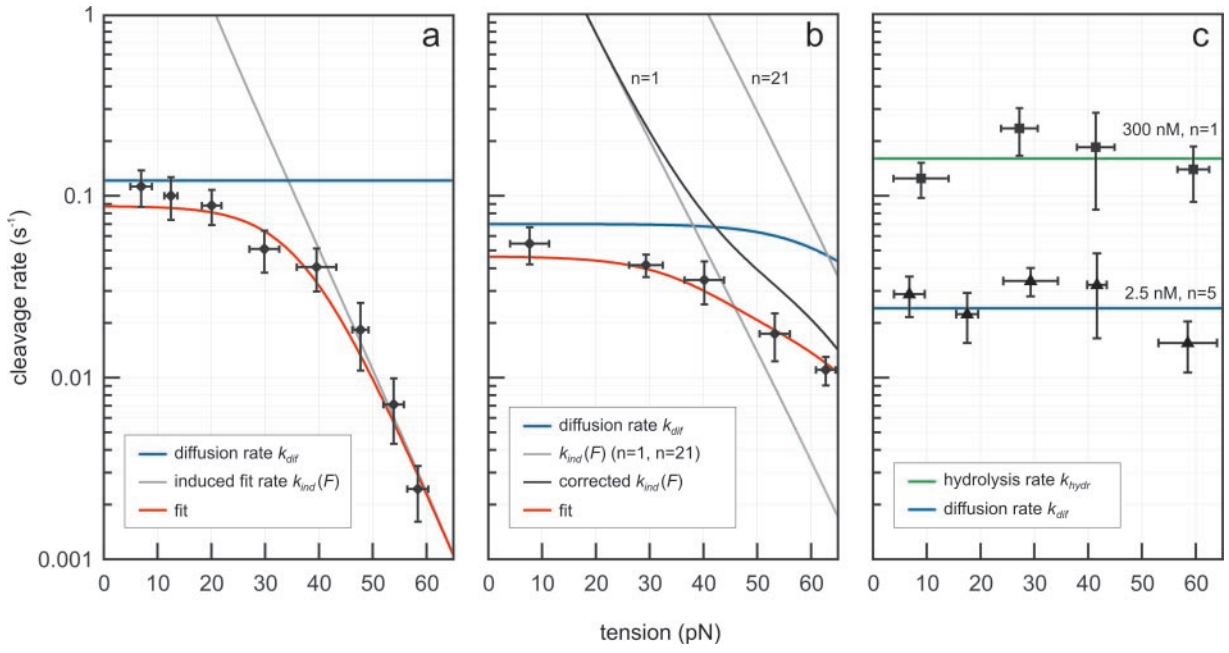


**Figure 5.** Measured cleavage rate versus DNA tension. (**a**) The effect of tension on cleavage of linearized *pCco5* by EcoRV (number of recognition sites $n = 1$). EcoRV concentration was 25 nM in terms of dimers. The total amount of cutting events was 68. (**b**) EcoRV on Lambda phage DNA ($n = 21$), 32 cutting events. (**c**) Tension dependence on DNA cleavage by BamHI (300 nM) on the *pCco5* derivative containing a single recognition site (squares, 78 events) and on Lambda phage DNA with five BamHI sites (triangles, 28 events) using 2.5 nM BamHI. Each point consists of at least 6 cleavage events. Vertical error bars represent the standard error of the mean rate. Horizontal error bars are the standard deviation of the combined DNA tensions (a result of the binning). The data in (a and b) are fitted to the described model (normalized $\chi^2$ are 0.6 and 0.2, respectively). The BamHI rates in (c) do not significantly vary with DNA tension and were fitted with constant values [normalized $\chi^2$ are 0.8 (hydrolysis, green line) and 1.6 (diffusion, blue line)].

semi-flexible polymers (38) and minimizing the total required energy (see Appendix).

Combining these three terms, the total change in free energy, $\Delta\Delta G$, of specific complex formation as a function of DNA tension ($F$) can be expressed as:

$$\Delta\Delta G(F) = \frac{6a}{K}F^2 + 6a \cdot \left(1 - \cos\left(\frac{\theta}{2}\right)\right)F + \frac{\theta^2}{4}\sqrt{L_p k_b T}\sqrt{F}, \quad \mathbf{1}$$

Here, $6a$ is the relaxed length of the recognition site (6 bp spaced at 0.34 nm), $K$ the DNA stretch modulus (~1200 pN) (37), $\theta$ the enzyme-induced DNA bending, $L_p$ the persistence length of DNA [53 nm (39)] and $k_bT$ the thermal energy. When this free energy change acts on the transition toward specific binding, then the induced-fit rate as a function of DNA tension, $k_{ind}(F)$, can be related to the induced-fit rate on relaxed DNA, $k_{ind}(0)$, using Arrhenius' law (Figure 6b).

The observed cleavage rate $k_c(F)$ depends on $k_{ind}(F)$, the first-order association rate or diffusion rate of the enzyme to the specific site ($k_{dif}$) and DNA backbone hydrolysis for both strands ($k_{hydr}$):

$$k_c(F) = \left(\frac{1}{k_{dif}} + \frac{1}{k_{ind}(F)} + \frac{1}{k_{hydr}}\right)^{-1}, \quad \mathbf{2}$$

Because the DNA is kept under tension, enzyme dissociation after hydrolysis from at least one of the cleaved ends should be almost instantaneous (this is confirmed by data presented below). For this reason, the rate of product release has not been included in Equation 2.

To describe cleavage of DNA with multiple ($n$) sites, Equation 2 needs to be extended. For such molecules, whenever diffusion is the rate-limiting step in the reaction, association of the first enzyme proceeds $n$ times faster: $k_{dif}$ now becomes $n \cdot k_{dif}$. If tension causes the induced-fit rate $k_{ind}(F)$ to become rate-limiting, more enzymes ($x > 1$) can bind, but only the first cut is observed. The consequences are 2-fold. First, multiple bound enzymes result in an apparent acceleration of $k_{ind}(F)$ with a factor $x$. Second, the diffusion rate decreases as the number of occupied sites grows. The last enzyme to bind before cleavage takes place encounters $n - (x - 1)$ free sites. $x$ depends on DNA tension and can be approximated semi-empirically with

$$x = \frac{nm}{n+m};\ m(F) = \frac{1}{2}\frac{nk_{dif}}{k_{ind}(F)} + 1. \quad \mathbf{3}$$

These extensions can be included in Equation 2, resulting in an expression for $k_{c,n}$ ($n > 1$):

$$k_{c,n}(F) = \left(\frac{1}{xk_{ind}(F)} + \frac{1}{(n - (x-1))k_{dif}} + \frac{1}{k_{hydr}}\right)^{-1}. \quad \mathbf{4}$$

This expression is valid for $n \cdot k_{dif} < k_{hydr}$ and $x \lesssim n/2$. Equations 2 and 4 can be used for fitting the measured $k_c$ and have three free parameters: $k_{dif}$, $\theta$ and $k_{ind}(0)$.

### Determining association and hydrolysis rates

In the proposed model, diffusion and hydrolysis rates are both assumed to be independent of DNA tension. However, $k_{dif}$ should depend on enzyme concentration, while $k_{hydr}$ should not. These two rates can, therefore, be obtained separately

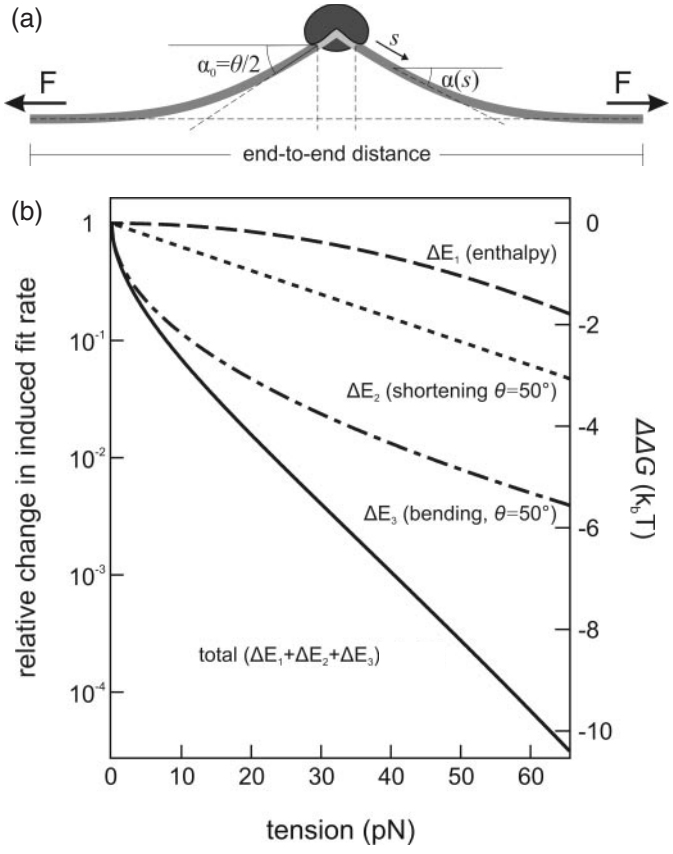


**Figure 6.** Mechanochemical model of tension dependence. (**a**) Schematic representation of DNA bending by a restriction enzyme under an applied external force. The enzyme induces a sharp kink in the DNA at the center of the recognition sequence. $\alpha_0$ is the half bend angle θ/2. (**b**) Theoretical model curves representing the effect of tension on the induced-fit rate using a bend angle θ = 50°. Dashed curve: overcoming the enthalpic stretching of the recognition sequence. Dotted curve: local shortening of the DNA end-to-end distance due to a kink at the center of the recognition site. Dashed–dotted curve: additional bending and end-to-end shortening of the DNA protruding from the enzyme–DNA complex. Solid curve: all three effects added, providing the dependence of the induced-fit rate on DNA tension.

(using this single-molecule technique) by measuring the cleavage rate as a function of enzyme concentration. Such measurements were performed with *pCco5* DNA for EcoRV concentrations ranging from 1 to 500 nM. During the assay, the DNA is kept at low tension (<10 pN) to ensure that the induced-fit mechanism is not rate-limiting. The results, displayed in Figure 7, show that the cleavage rate $k_c$ increases linearly with [EcoRV], but at high concentration it is dominated by hydrolysis ($k_{hydr}$) and levels off. The data are fitted with the following equation:

$$k_c = \left(\frac{1}{k_{hydr}} + \frac{1}{k_{on}[\mathrm{EcoRV}]}\right)^{-1}; \quad k_{dif} = k_{on}[\mathrm{EcoRV}], \qquad \mathbf{5}$$

resulting in a $k_{hydr}$ of 0.33 ± 0.05 $s^{-1}$ and an association rate $k_{on}$ of (4 ± 1) · $10^6$ $M^{-1}$ $s^{-1}$. The same numbers can also be obtained by looking at the distribution of individual cleavage events at a particular concentration. Figure 7b shows this distribution at high EcoRV concentration (500 nM), which can be fitted to a single exponential to determine the hydrolysis rate. At 25 nM EcoRV the association and hydrolysis rates are similar. The histogram in Figure 7c clearly displays a two-step process, from which both rates can be extracted. The measured hydrolysis rate is in good agreement with the reported values for EcoRV (24,25,40,41). This result also justifies our assumption that in these single-molecule experiments product release after hydrolysis is fast. The association rate we acquired, however, is ~25 times lower than that obtained in biochemical studies under optimal conditions (~$10^8$ $M^{-1}$ $s^{-1}$) (17,24,26,40). It is generally believed that site-specific DNA enzymes find their target sequences via 'facilitated diffusion', thereby accelerating the search process. Several mechanisms for facilitated diffusion have been suggested (9–11,19,20): (i) 'sliding', proteins performing a 1D random walk along the DNA contour, (ii) 'hopping', fast dissociation and re-association from one nearby site to another and (iii) 'jumping', transfer between non-specific DNA sites close to each other in 3D space yet separated by large distances along the DNA contour. In bulk studies and *in vivo* long DNA molecules have a globular shape; many sites that are distant in 1D space are close together in 3D space. In our single-molecule experiments, the DNA suspended between beads is in a completely different geometry: it is fully stretched, even at a few pN of tension. Such an arrangement does not *per se* influence sliding and hopping, but should drastically inhibit jumping. The *pCco5* DNA substrate (6538 bp) used in the experiments is much larger than the average number of base pairs scanned by an individual enzyme in one binding event. Hence, several rebinding events (jumps) are necessary to locate the target sequence. For stretched DNA, the local 'density' of DNA sites is much lower than for DNA having a globular shape. Therefore, in the stretched case the chance for an enzyme to, after dissociation from non-specific DNA, rebind via 3D pathways to an uncorrelated site anywhere on the DNA molecule is much smaller than for relaxed DNA. This effect seems to be reflected in the reduced association rate of (4 ± 1) · $10^6$ $M^{-1}$ $s^{-1}$ we observe for EcoRV on stretched DNA.

## Cleaving DNA under tension with EcoRV

With the association rate of EcoRV on *pCco5* in our experiments known, $k_{dif}$ in Equation 2 can be fixed at 0.1 ± 0.025 $s^{-1}$ (for 25 nM EcoRV). Fitting $k_c$ data results in: θ = 54° ± 6° and $k_{ind}(0)$ between 35 and 1000 $s^{-1}$ (Figure 5a). The obtained bend angle is in good agreement with crystal structures (50°–60°) (2,18,33) and somewhat higher than observed in gel retardation experiments (44° ± 4°) (42,43). The uncertainty in $k_{ind}(0)$ stems from extrapolating $k_{ind}(F)$ back to zero force and a significant correlation in the model between $k_{ind}(0)$ and θ. Combining this data with that of Hiller *et al*. (17), who determined $k_{ind}(0)$ to be at least 100 $s^{-1}$ (based on the dead time of the instrument used), confines the induced-fit rate $k_{ind}(0)$ between 100 and 1000 $s^{-1}$. Such a rate is comparable with that of other induced-fit reactions on DNA, such as DNA polymerase (44).

EcoRV cleavage rates on Lambda phage DNA ($n = 21$) were measured with a 10 times lower enzyme concentration than the *pCco5* experiments, in order to compensate for the increased diffusion rate ($n \cdot k_{dif}$) and so keeping the cutting time above the time resolution of our instrument. The data (Figure 5b) were fitted with Equation 4 and resulted in $n \cdot k_{dif}$ of 0.07 ± 0.02 $s^{-1}$, corresponding with an average association rate per

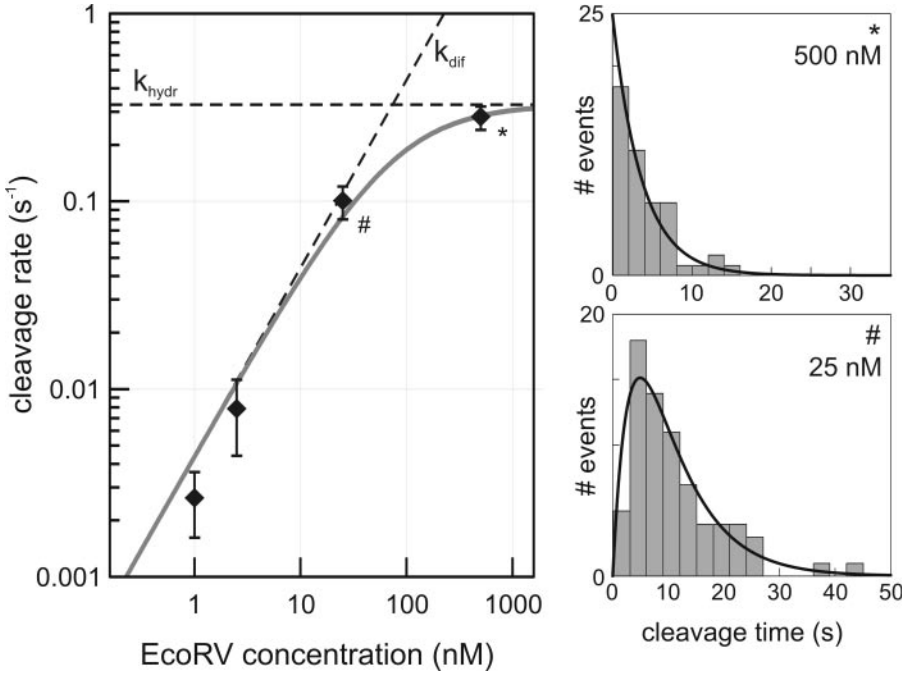


**Figure 7.** EcoRV concentration dependence of the cleavage rate. (**a**) Cleavage of *pCco5* DNA (one recognition sequence) by EcoRV for different enzyme concentrations. Cleavage rates were obtained at low DNA tensions (<10 pN) to ensure that the induced-fit mechanism was not rate-limiting. A total of 157 events were measured. Error bars represent the standard error of the mean rate for each of the concentrations. (**b**) Distribution of the single-molecule cleavage reaction times of the averaged data point indicated with asterisk in (a) (51 cleavage events). The EcoRV concentration (500 nM) is such that hydrolysis only is the rate-limiting step. Hence, an exponential distribution is expected. This is indeed observed. The hydrolysis rate obtained by fitting an exponential (solid curve) is $0.27 \pm 0.05$ s$^{-1}$ ($\chi^2 = 0.7$). (**c**) Histogram of cleavage events of the averaged data point indicated with hash in (a) (73 reactions). This distribution displays a two-step process. At 25 nM EcoRV association and hydrolysis are of the same order of magnitude. Both processes by themselves obey Poissonian statistics and follow exponential distributions. However, as hydrolysis can only occur after binding, they are not independent. The distribution is thus fit with a convolution of two exponentials ($\chi^2 = 0.7$). The rates found for association and hydrolysis are $0.13 \pm 0.03$ s$^{-1}$ [$k_{on} = (5 \pm 1) \cdot 10^6$ M$^{-1}$ s$^{-1}$] and $0.29 \pm 0.09$ s$^{-1}$, respectively. Both rates are identical to the rates found by fitting Equation 5 to the data points in (a).

recognition site of $1 \times 10^6$ M$^{-1}$ s$^{-1}$, slightly less than that determined for *pCco5*. Note that at high forces fewer sites are available and the diffusion rate decreases. The obtained bend angle is $52° \pm 9$. The weaker dependence of $k_c$ on DNA tension in these multiple-site experiments results in a larger range (between 10 and 2000 s$^{-1}$) for $k_{ind}(0)$. These results nevertheless confirm the robustness of the experiments: different enzyme concentrations, DNA molecules and different number of sites lead to similar fit parameters.

### Cleaving DNA under tension with BamHI

In contrast to EcoRV, cleavage by 300 nM BamHI of a *pCco5* derivative ($n = 1$) remains largely unaffected by DNA tension (Figure 5c, squares). Therefore, we fitted these data with a constant value instead of Equation 2. This independence of force can be expected from the crystal structures of BamHI, which show that the DNA conformation is virtually unchanged upon specific binding (3,23). Hence, only the first term in Equation 1 has an effect on $k_{ind}$ and reduces this rate less than one order of magnitude. Consequently, $k_{ind}(0)$ should be faster than 10 s$^{-1}$ in order to explain the data, not unexpected considering the rate obtained for EcoRV. The BamHI concentration used in these experiments is sufficiently high so that, even with a 25-fold reduced association rate as found for EcoRV, hydrolysis should be rate-limiting. This is confirmed, since the cleavage rate $k_c$ obtained by fitting, $0.14 \pm 0.02$ s$^{-1}$, is comparable with the reported $k_{hydr}$ of BamHI [0.23 s$^{-1}$ for both DNA strands (4)]. Interestingly, these results show that the hydrolysis reaction is not measurably affected by DNA tension. The DNA inside the binding pocket is thus shielded from the tension and the energetic cost of cleaving mechanically constrained DNA is fully paid during the induced-fit reaction.

No force dependence of $k_c$ was detected in cleavage experiments using 2.5 nM BamHI on Lambda phage DNA ($n = 5$) (Figure 5c, triangles). At this concentration, diffusion to a target site is rate-limiting and the measured $k_c$, $0.024 \pm 0.003$ s$^{-1}$, therefore represents $n \cdot k_{dif}$. This corresponds to an association rate $k_{on}$ per site of $2 \times 10^6$ M$^{-1}$ s$^{-1}$, again reflecting the disappearance of jumping, as found for EcoRV. Finally, these experiments show that enthalpic stretching of the DNA [at forces beyond the suppressed jumping (>1 pN)] has no significant additional influence on locating the specific site ($k_{dif}$). A further reduction in association rate due to a decrease in binding affinity would have manifested itself in a slower observed cleavage rate for higher tensions, which is not the case. This result and the tension insensitive hydrolysis both support the assumptions made in the model.

## DISCUSSION

The profound difference in sensitivity to DNA tension between EcoRV and BamHI is shown to be a direct result of the dissimilarity in the induced-fit reaction between the two enzymes;

EcoRV strongly bends the DNA while BamHI does not. From the mechanochemical model, it is also clear that the energetic cost of bending DNA under tension is high, since the semi-flexible nature of DNA increases the bent region far beyond the actual binding site. In fact, at high force $\Delta\Delta G$ depends mostly on the square of the bend angle $\theta$ (Equation 1 and Figure 6b). The enzyme must deliver this extra work during the formation of the specific complex. The only tension dependence of DNA cleavage by BamHI is the energy cost of the increased base pair spacing. Even at the highest tension (the overstretching force), this effect does not modulate the induced-fit rate enough to make this step rate-limiting.

The model used to describe the effect of DNA tension on EcoRV and BamHI is applicable to other type II restriction enzymes. However, the insensitive induced-fit rate of BamHI also points out a limitation: it is only possible to obtain bend angles and induced-fit rates if DNA tension can make this last process rate-limiting, i.e. slower than the hydrolysis rate in optimal conditions. Such a reduction is possible if an enzyme induces a bend or kink in the DNA larger than some critical angle (estimated to be $\sim 35^\circ$). So, although changes in $\Delta G$ as small as $\sim 0.5\ k_bT$ can be distinguished, only the rate-limiting step can be monitored.

In a recent paper, it has been shown that EcoRV cleaves long supercoiled plasmids faster than relaxed ones (12). The authors explained this preference by stating that the enzyme is guided more quickly to its target sequence because the higher compactness of the DNA allowed more 3D transfers (i.e. jumping) between non-specific sites. The strong decrease in association rate we find on stretched DNA directly outlines and quantifies the importance of these 3D pathways to locate a specific site. Directly managing the DNA configuration by pulling the ends apart allows a controlled and complete shut-down of jumping, without altering sliding and hopping. Future experiments systematically investigating the relation between DNA density and jumping might provide new insights in this important mechanism.

The shielding of the DNA inside the binding pocket as demonstrated for BamHI and inferred in EcoRV is probably a direct result of the specificity of the binding. Only the correct sequence should lead to an induced-fit reaction, but elastically stretched DNA is slightly deformed. Therefore, the induced-fit forces the DNA in normal (zero tension) configuration. Once the enzyme is properly bound, the DNA inside the binding pocket is no longer under tension and hydrolysis should occur with normal rate. These effects of tension on jumping and hydrolysis reported here should be generic for any specific DNA binding protein since they all use similar strategies for finding and recognizing their site.

Finally, the strong coupling between DNA tension and the ability to bend DNA as demonstrated and modeled in this study is expected to be valid for any DNA-bending protein (specific or not). A similar coupling has also been indirectly shown for specific binding by RNA polymerase (45). Therefore, tension naturally occurring on DNA stretches during the constant reordering of DNA within cells should disfavor binding of DNA-bending proteins. Such regulatory mechanism has not been appreciated before and could be, in particular, relevant for gene regulation. Future experiments could test these hypotheses by using other restriction enzymes and their mutant forms, regulatory proteins and polymerases, in order to find and compare association, hydrolysis and induced-fit rates as well as possible bend angles.

## ACKNOWLEDGEMENTS

The authors thank J. J. Perona for stimulating discussions and the kind gift of EcoRV enzyme, W. Reijnders for kindly providing DNA Plasmid *pCco5*, J. van Mameren and E. J. G. Peterman for their helpful ideas and suggestions, and thanks to C. F. Schmidt for providing the opportunity to start experiments on his instrumentation. G.J.L.W. conceived the experiment; M.C.N. and B.v.d.B. constructed the setup; B.v.d.B. carried out the experiments and, together with G.J.L.W., developed the model and wrote the paper. This work was supported by an NWO Vernieuwingsimpuls grant and by a grant from the Dutch Foundation of Fundamental Research on Matter (FOM) (to G.J.L.W.). Funding to pay the Open Access publication charges for this article was provided by the Vrije Universiteit, Amsterdam.

*Conflict of interest statement*. None declared.

## REFERENCES

1. Taylor,J.D. and Halford,S.E. (1989) Discrimination between DNA sequences by the EcoRV restriction endonuclease. *Biochemistry*, **28**, 6198–6207.
2. Winkler,F.K., Banner,D.W., Oefner,C., Tsernoglou,D., Brown,R.S., Heathman,S.P., Bryan,R.K., Martin,P.D., Petratos,K. and Wilson,K.S. (1993) The crystal structure of EcoRV endonuclease and of its complexes with cognate and non-cognate DNA fragments. *EMBO J.*, **12**, 1781–1795.
3. Viadiu,H. and Aggarwal,A.K. (2000) Structure of BamHI bound to nonspecific DNA: a model for DNA sliding. *Mol. Cell*, **5**, 889–895.
4. Engler,L.E., Sapienza,P., Dorner,L.F., Kucera,R., Schildkraut,I. and Jen-Jacobson,L. (2001) The energetics of the interaction of BamHI endonuclease with its recognition site GGATCC. *J. Mol. Biol.*, **307**, 619–636.
5. Lesser,D.R., Kurpiewski,M.R. and Jen-Jacobson,L. (1990) The energetic basis of specificity in the Eco RI endonuclease–DNA interaction. *Science*, **250**, 776–786.
6. Thielking,V., Alves,J., Fliess,A., Maass,G. and Pingoud,A. (1990) Accuracy of the EcoRI restriction endonuclease: binding and cleavage studies with oligodeoxynucleotide substrates containing degenerate recognition sequences. *Biochemistry*, **29**, 4682–4691.
7. Taylor,J.D. and Halford,S.E. (1992) The activity of the EcoRV restriction endonuclease is influenced by flanking DNA sequences both inside and outside the DNA–protein complex. *Biochemistry*, **31**, 90–97.
8. Jeltsch,A., Wenz,C., Stahl,F. and Pingoud,A. (1996) Linear diffusion of the restriction endonuclease EcoRV on DNA is essential for the *in vivo* function of the enzyme. *EMBO J.*, **15**, 5104–5111.
9. Berg,O.G., Winter,R.B. and von Hippel,P.H. (1981) Diffusion-driven mechanisms of protein translocation on nucleic acids. 1. Models and theory. *Biochemistry*, **20**, 6929–6948.
10. von Hippel,P.H. and Berg,O.G. (1989) Facilitated target location in biological systems. *J. Biol. Chem.*, **264**, 675–678.
11. Halford,S.E. (2001) Hopping, jumping and looping by restriction enzymes. *Biochem. Soc. Trans.*, **29**, 363–374.
12. Gowers,D.M. and Halford,S.E. (2003) Protein motion from non-specific to specific DNA by three-dimensional routes aided by supercoiling. *EMBO J.*, **22**, 1410–1418.
13. Halford,S.E. and Marko,J.F. (2004) How do site-specific DNA-binding proteins find their targets? *Nucleic Acids Res*, **32**, 3040–3052.
14. Taylor,J.D., Badcoe,I.G., Clarke,A.R. and Halford,S.E. (1991) EcoRV restriction endonuclease binds all DNA sequences with equal affinity. *Biochemistry*, **30**, 8743–8753.
15. Martin,A.M., Horton,N.C., Lusetti,S., Reich,N.O. and Perona,J.J. (1999) Divalent metal dependence of site-specific DNA binding by EcoRV endonuclease. *Biochemistry*, **38**, 8430–8439.

16. Martin,A.M., Sam,M.D., Reich,N.O. and Perona,J.J. (1999) Structural and energetic origins of indirect readout in site-specific DNA cleavage by a restriction endonuclease. *Nature Struct. Biol.*, **6**, 269–277.
17. Hiller,D.A., Fogg,J.M., Martin,A.M., Beechem,J.M., Reich,N.O. and Perona,J.J. (2003) Simultaneous DNA binding and bending by EcoRV endonuclease observed by real-time fluorescence. *Biochemistry*, **42**, 14375–14385.
18. Horton,N.C. and Perona,J.J. (2000) Crystallographic snapshots along a protein-induced DNA-bending pathway. *Proc. Natl Acad. Sci. USA*, **97**, 5729–5734.
19. Stanford,N.P., Szczelkun,M.D., Marko,J.F. and Halford,S.E. (2000) One- and three-dimensional pathways for proteins to reach specific DNA sites. *EMBO J.*, **19**, 6546–6557.
20. Halford,S.E. and Szczelkun,M.D. (2002) How to get from A to B: strategies for analysing protein motion on DNA. *Eur. Biophys. J.*, **31**, 257–267.
21. Halford,S.E. and Goodall,A.J. (1988) Modes of DNA cleavage by the EcoRV restriction endonuclease. *Biochemistry*, **27**, 1771–1777.
22. Newman,M., Strzelecka,T., Dorner,L.F., Schildkraut,I. and Aggarwal,A.K. (1994) Structure of restriction endonuclease BamHI and its relationship to EcoRI. *Nature*, **368**, 660–664.
23. Newman,M., Strzelecka,T., Dorner,L.F., Schildkraut,I. and Aggarwal,A.K. (1995) Structure of Bam HI endonuclease bound to DNA: partial folding and unfolding on DNA binding. *Science*, **269**, 656–663.
24. Baldwin,G.S., Vipond,I.B. and Halford,S.E. (1995) Rapid reaction analysis of the catalytic cycle of the EcoRV restriction endonuclease. *Biochemistry*, **34**, 705–714.
25. Engler,L.E., Welch,K.K. and Jen-Jacobson,L. (1997) Specific binding by EcoRV endonuclease to its DNA recognition site GATATC. *J. Mol. Biol.*, **269**, 82–101.
26. Erskine,S.G., Baldwin,G.S. and Halford,S.E. (1997) Rapid-reaction analysis of plasmid DNA cleavage by the EcoRV restriction endonuclease. *Biochemistry*, **36**, 7567–7576.
27. Stanford,N.P., Halford,S.E. and Baldwin,G.S. (1999) DNA cleavage by the EcoRV restriction endonuclease: pH dependence and proton transfers in catalysis. *J. Mol. Biol.*, **288**, 105–116.
28. Davenport,R.J., Wuite,G.J.L., Landick,R. and Bustamante,C. (2000) Single-molecule study of transcriptional pausing and arrest by *E.coli* RNA polymerase. *Science*, **287**, 2497–2500.
29. Wuite,G.J.L., Smith,S.B., Young,M., Keller,D. and Bustamante,C. (2000) Single-molecule studies of the effect of template tension on T7 DNA polymerase activity. *Nature*, **404**, 103–106.
30. Strick,T.R., Croquette,V. and Bensimon,D. (2000) Single-molecule analysis of DNA uncoiling by a type II topoisomerase. *Nature*, **404**, 901–904.
31. Smith,D.E., Tans,S.J., Smith,S.B., Grimes,S., Anderson,D.L. and Bustamante,C. (2001) The bacteriophage straight phi29 portal motor can package DNA against a large internal force. *Nature*, **413**, 748–752.
32. Wang,M.D., Schnitzer,M.J., Yin,H., Landick,R., Gelles,J. and Block,S.M. (1998) Force and velocity measured for single molecules of RNA polymerase. *Science*, **282**, 902–907.
33. Perona,J.J. and Martin,A.M. (1997) Conformational transitions and structural deformability of EcoRV endonuclease revealed by crystallographic analysis. *J. Mol. Biol.*, **273**, 207–225.
34. Svoboda,K. and Block,S.M. (1994) Biological applications of optical forces. *Annu. Rev. Biophys. Biomol. Struct.*, **23**, 247–285.
35. Wuite,G.J.L., Davenport,R.J., Rappaport,A. and Bustamante,C. (2000) An integrated laser trap/flow control video microscope for the study of single biomolecules. *Biophys. J.*, **79**, 1155–1167.
36. Smith,S.B., Cui,Y. and Bustamante,C. (1996) Overstretching B-DNA: the elastic response of individual double-stranded and single-stranded DNA molecules. *Science*, **271**, 795–799.
37. Odijk,T. (1995) Stiff chains and filaments under tension. *Macromolecules*, **28**, 7016–7018.
38. Marko,J.F. and Siggia,E.D. (1995) Stretching DNA. *Macromolecules*, **28**, 8759–8770.
39. Bustamante,C., Marko,J.F., Siggia,E.D. and Smith,S. (1994) Entropic elasticity of lambda-phage DNA. *Science*, **265**, 1599–1600.
40. Erskine,S.G. and Halford,S.E. (1998) Reactions of the EcoRV restriction endonuclease with fluorescent oligodeoxynucleotides: identical equilibrium constants for binding to specific and non-specific DNA. *J. Mol. Biol.*, **275**, 759–772.
41. Sam,M.D. and Perona,J.J. (1999) Catalytic roles of divalent metal ions in phosphoryl transfer by EcoRV endonuclease. *Biochemistry*, **38**, 6576–6586.
42. Stover,T., Kohler,E., Fagin,U., Wende,W., Wolfes,H. and Pingoud,A. (1993) Determination of the DNA bend angle induced by the restriction endonuclease EcoRV in the presence of $Mg^{2+}$. *J. Biol. Chem.*, **268**, 8645–8650.
43. Cal,S. and Connolly,B.A. (1996) The EcoRV modification methylase causes considerable bending of DNA upon binding to its recognition sequence GATATC. *J. Biol. Chem.*, **271**, 1008–1015.
44. Patel,S.S., Wong,I. and Johnson,K.A. (1991) Pre-steady-state kinetic analysis of processive DNA replication including complete characterization of an exonuclease-deficient mutant. *Biochemistry*, **30**, 511–525.
45. Harada,Y., Funatsu,T., Murakami,K., Nonoyama,Y., Ishihama,A. and Yanagida,T. (1999) Single-molecule imaging of RNA polymerase–DNA interactions in real time. *Biophys. J.*, **76**, 709–715.
46. Lai,P. and Zhou,Z. (2001) Worm-like chain under an external force: a classical mechanical approach. *Chinese Journal of Physics*, **39**, 641–650.

## APPENDIX

### Calculation of free energy changes in specific binding due to DNA tension

Three independent contributions that change the free energy $\Delta G$ for specific complex formation as a function of force were assumed:

(i) The distance between adjacent base pairs increases when DNA is put under tension. This elongation is incorporated in the worm-like chain model for semi-flexible polymers by the introduction of the stretch modulus ($K$) (37). The enzyme must compress the DNA at the recognition site against an applied force ($F$) to normal base pair spacing ($a$). The associated energy cost can be expressed as:

$$\Delta E_1 = l \cdot a \cdot \left(\frac{F}{K}\right) F, \qquad \text{A1}$$

where $l$ is the number of base pairs with intimate DNA–enzyme contact ($l \cdot a$ is the length of the DNA sequence with intimate contact; $l = 6$ for EcoRV and BamHI).

(ii) Some restriction enzymes, such as EcoRV, kink DNA by an angle $\theta = 2\alpha_0$ at the recognition site. This kink within the binding pocket leads to a direct shortening of the end-to-end distance against the applied force (Figure 6a). The required work is given by:

$$\Delta E_2 = l \cdot a \cdot \left(1 - \cos\left(\frac{\theta}{2}\right)\right) F. \qquad \text{A2}$$

(iii) The amount of DNA bending plus shortening outside the complex depends on the tension and the bend angle $\theta$ (Figure 6a). The free energy cost of this effect is found by calculating the lowest energy DNA configuration using the worm-like chain model (38,46). Given a kink of angle $\theta = 2\alpha_0$ in the middle of the polymer with length $L$ with a bending modulus $\kappa = L_p k_b T$, the expression becomes

$$\Delta E_3 = 2 \int_0^{L/2} \left(\frac{\kappa}{2}\left(\frac{\mathrm{d}\alpha(s)}{\mathrm{d}s}\right)^2 + F(1 - \cos\alpha(s))\right) \mathrm{d}s. \qquad \text{A3}$$

Here, the first term in the integrand represents the bending energy, with $\mathrm{d}\alpha(s)/\mathrm{d}s = 1/R(s)$ the local curvature at position

*s* on the DNA. The second term is the potential energy stored in the system due to the shortening of end-to-end distance against the force. (The force will actually slightly increase due to this movement. This effect is, however, negligible. In fact the end-to-end shortening will partition itself between bead displacement in the traps and extension of the DNA, depending on the relative stiffness of the two. Nevertheless, the associated energy difference is the same.) Equation A3 can be solved by treating the integrand $Z$ in the right-hand side as the Lagrangian of an action potential $E$ and applying the principle of least action. This leads to the Euler–Lagrange differential equation

$$\frac{\mathrm{d}}{\mathrm{d}s}\left(\frac{\delta Z}{\delta \dot{\alpha}(s)}\right) - \frac{\delta Z}{\delta \alpha(s)} = 0 \Rightarrow \kappa \frac{\mathrm{d}^2\alpha(s)}{\mathrm{d}s^2} + F\sin\alpha(s) = 0. \quad \textbf{A4}$$

This is the equation of motion for a harmonic oscillator with large amplitude. It can be solved using elliptic integrals, but for small bend angles can be greatly simplified by taking $\sin\alpha(s) \approx \alpha(s)$. For EcoRV ($\alpha_0 = 25^\circ$) this results in an error of a few percent. Solving Equation A4 and performing the integral yields

$$\Delta E_3 = \alpha_0^2\sqrt{\kappa F} = \alpha_0^2\sqrt{L_\mathrm{p}k_bT}\sqrt{F} = \frac{\theta^2}{4}\sqrt{L_\mathrm{p}k_bT}\sqrt{F}. \quad \textbf{A5}$$

This is the energy cost of bending the DNA plus the work associated with the end-to-end distance shortening due to this bending.